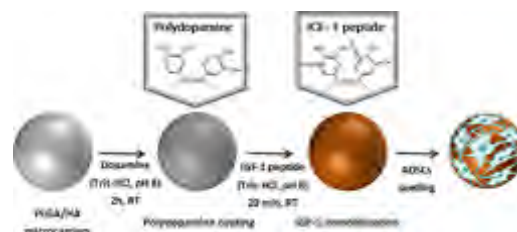


Biodegradable Microcarriers of Poly(Lactide-co-Glycolide) and Nano-Hydroxyapatite Decorated with IGF-1 via Polydopamine Coating for Enhancing Cell Proliferation and Osteogenic Differentiation

Tianlin Gao, Ning Zhang, Zongliang Wang, Yu Wang, Ya Liu,* Yoshihiro Ito, Peibiao Zhang*

In this study, insulin-like growth factor 1 (IGF-1) was successfully immobilized on the poly (lactide-co-glycolide)/hydroxyapatite (PLGA/HA) and pure PLGA microcarriers via polydopamine (pDA). The results demonstrated that the pDA layer facilitated simple and highly efficient immobilization of peptides on the microcarriers within 20 min. Mouse adipose-derived stem cells (ADSCs) attachment and proliferation on IGF-1-immobilized microcarriers were much higher than non-immobilized ones. More importantly, the IGF-1-immobilized PLGA/HA microcarriers significantly increased alkaline phosphatase (ALP) activity and expression of osteogenesis-related genes of ADSCs. Therefore, it is considered that the IGF-1-decorated PLGA/HA microcarriers will be of great value in the bone tissue engineering.



1. Introduction

Bone defects, originated from trauma, tumor resection, infection, and skeletal abnormalities, put a great need of bone grafts, including autografts, allografts, and xenografts, which have been widely applied on bone repair.^[1,2] Although some of the grafts are effective for bone

regeneration, many drawbacks have limited their development, such as immune reaction, limited availability, transfer of pathogens, and non-biodegradability.^[3] Meanwhile, it appears to be the most promising alternative to existing therapies for bone repair and regeneration by using osteogenic cells, osteoinductive growth factors, and scaffolds alone or in combination.^[4] One of the most

T. Gao, Y. Liu
School of Public Health, Jilin University, Changchun 130021,
P. R. China
E-mail: liuya@jlu.edu.cn

T. Gao, Z. Wang, Y. Wang, P. Zhang
Key Laboratory of Polymer Ecomaterials, Changchun Institute of
Applied Chemistry, Chinese Academy of Sciences, Changchun
130022, P. R. China
E-mail: zhangpb@ciac.ac.cn

N. Zhang
Department of Foot and Ankle Surgery, The Second Hospital of
Shandong University, Jinan 250000, P. R. China
Y. Ito
Nano Medical Engineering Laboratory, RIKEN, 2-1-Hirosawa,
Wako, Saitama 351-0198, Japan
Emergent Bioengineering Materials Research Team, RIKEN Center
for Emergent Materials Science, 2-1-Hirosawa, Wako, Saitama
351-0198, Japan

significant challenges is to design and fabricate a biomimetic cell-loaded scaffold that can be directly applied on bone repair.

Recently, much attention has been paid to microcarriers composed of biodegradable polymers,^[5,6] such as poly(lactide) (PLA),^[7] poly(glycolide) (PGA), and their copolymer poly(lactide-co-glycolide) (PLGA), since the polymers possess good mechanical properties, low immunogenicity and toxicity, and an adjustable degradation rate.^[8,9] The biodegradable microcarriers not only provide a large number of cells for the field of cell therapy but also can be directly applied on tissue and organ as microcarriers/cells compound without enzyme treatment and harvest.^[3,9] PLGA is one kind of the most promising degradable materials in tissue engineering because their degradation rate can be adjusted by altering the ratio of lactic to glycolic acids.^[10] However, hydrophobic properties and lack of bioactivity seriously limit its biological applications. Hydroxyapatite ($\text{Ca}_{10}(\text{PO}_4)_6(\text{OH})_2$, HA) is an effective component for biomimetic materials because of its similarity with the mineral phase of natural bone. It has the abilities of bone binding and osteoconductivity and has been widely used in bone tissue engineering.^[11] Considering that microcarriers exhibit good flowability and can be employed as a three-dimensional scaffold to be injected into various shaped bone defects for bone repair, PLGA/HA composite microcarriers could provide more versatile applications than pre-shaped scaffolds.^[3]

In addition, microcarriers can have the ability to induce stem cells differentiation when loading growth factors, peptides, or drugs et al. Modification with growth factors or other bioactive molecules can compensate for the lack of osteogenic potential of synthetic polymer.^[12] Insulin-like growth factor 1 (IGF-1) has gained interest as a therapeutic factor in fracture healing, either alone or in combination with other growth factors.^[13–15] IGF-1, as somatomedin C and somatomedin A, is a mitogenic factor that enhances growth in adult cells as well as aids in embryonic growth and differentiation.^[16] It has been shown to enhance proliferation of mesenchymal stem cells and reverse the suppression of osteogenic differentiation by implants.^[17] Furthermore, poly(D,L-lactide) incorporated with IGF-1 and TGF- β can accelerate rats fracture healing significantly without systemic side-effects.^[18] But few works have been reported about the combined effect of HA and IGF-1 on bone tissue engineering. And it is speculated that if we utilized some methods to immobilize IGF-1 on the microcarriers, the IGF-1-immobilized microcarriers could not only help the proliferation of desired cells but also help the cells osteoinductive.

Inspired by mussels' adhesive mechanism, a versatile polydopamine (pDA)-coating method was recently created by simply dipping a substrate into an alkaline

dopamine (DA) solution.^[19] In an alkaline environment, the catechol groups of DA were oxidized to form a pDA ad-layer on a wide range of organic and inorganic materials, such as polymers, metals, and metal oxides.^[20–22] It is more simple than other chemical conjugation methods which usually require multistep, complicated procedures such as pretreatment of oxygen plasma,^[23] irradiation,^[24] chemicals,^[25] or surface activation.^[4] It is reported that the pDA coating on the surface of materials could be divided into two steps. At the beginning, oxidation and rearrangement of DA could occur in alkaline solutions, resulting in 5,6-dihydroxyindole, which is the monomer for polymerization in the following step.^[26] Cyclization of amino group ($-\text{NH}_2$) could take place and hydroxyl ($-\text{OH}$) groups could remain for the polymer after this reaction.^[27,28] It is well known that the hydroxyl group containing compounds always liberate hydrogen cations and make the parent compound an acid. The functional groups (i.e. $-\text{CO}-$, $-\text{OH}$) of PLGA and HA could help induce the occurrence of DA polymerization on the surface of substances and further promote the formation of an even coating of pDA.^[26] Interestingly, it has been proved that pDA coating could promote the adhesion of certain cell types to various surfaces due to an increase in immobilization of serum adhesive proteins.^[29] We speculate that this simple technique is suitable for conjugation of bioactive factors, like IGF-1, on PLGA microcarriers to prepare functional biodegradable microcarriers.

The objective of this study was to investigate the enhanced bioactivity and osteoinductivity of PLGA/HA microcarriers with IGF-1 immobilization via pDA coating. The microcarriers were fabricated by O/W emulsion, and pDA was coated on the microcarriers to immobilize the IGF-1. CCK-8 assay and cytoskeleton staining were operated to determine the attachment and growth promotion of adipose-derived stem cells (ADSCs) on the functional microcarriers. Then, alkaline phosphatase (ALP) activity and quantitative real-time polymerase chain reaction (qRT-PCR) were performed to explore the osteoinductive effect of the microcarriers.

2. Experimental Section

2.1. Materials

PLGA (lactide/glycolide ratio = 80/20, Mn = 85 000) was synthesized by Changchun Institute of Applied Chemistry, Chinese Academy of Sciences (CIAC, China). Polyvinyl alcohol (PVA, Alcoholysis 99.8–100% (mol/mol) was purchased from Aladdin Chemistry Co. Ltd. Dichloromethane (DCM) was obtained from Beijing Chemical Works. Recombinant Human IGF-1 was purchased from UB Biotech. Co. Ltd. 3-Hydroxytyramine hydrochloride was purchased from Adamas Reagent Co. Ltd.

2.2. Preparation of PLGA/HA Microcarriers

HA nanoparticles were synthesized as our previous work.^[30] Then, PLGA/HA microcarriers were prepared as followed. 0.07 g HA were dispersed in 1 mL DCM and 0.63 g PLGA were dissolved in 9 mL DCM. Then, the HA suspension was dropped into PLGA solution and subsequently stirred at 500 rpm for 24 h. The total solids content of HA was 10% (w/w). The final mixture was poured into a rapidly stirring PVA solution (150 mL, 2% (w/v)) at 400 rpm and then stirred overnight to allow the solvent evaporation. The PVA solution was decanted off and the microcarriers were washed three times in distilled water. Pure PLGA microcarriers were also prepared at the same conditions.

2.3. pDA Coating and IGF-1 Immobilization

The pDA coating was performed as followed. PLGA/HA microcarriers and PLGA microcarriers were immersed in a DA solution ($2 \text{ mg} \cdot \text{mL}^{-1}$ in 10 mM Tris-HCL, pH 8) and placed on a shaker for 2 h at room temperature (pDA @ PLGA/HA and pDA @ PLGA). The pDA-coated microcarriers were then rinsed with distilled water for five times to remove unattached DA molecules. After that, IGF-1 was immobilized onto pDA @ PLGA/HA and pDA @ PLGA (pDA @ PLGA/HA/IGF-1 and pDA @ PLGA/IGF-1). The pDA-coated microcarriers (50 mg for each group) were immersed in IGF-1 solution (10 mL) with different concentrations of 1, 10, and $100 \text{ ng} \cdot \text{mL}^{-1}$ for 20 min at room temperature. The microcarriers were then washed with distilled water for three times to remove the unattached peptides.

2.4. Analyses of Microcarriers

A scanning electron microscope (SEM, XL30 ESEM-FEG, FEI) was used to observe the morphology and the surface topography of the microcarriers. Microcarrier samples were frozen-dried, mounted on metal stubs with double sided tape, and coated with chromium. Energy-dispersive X-ray spectroscopy (EDX) was used in conjunction with SEM for elemental analysis of the mineral crystals.

Fourier transform infrared spectroscopy (FT-IR, Perkin Elmer, FTIR-2000) was used to determine the chemical structure of the microcarriers before and after soaking in pDA solution.

2.5. Immobilization of Lysozyme

Lysozyme was selected as a model protein to determine the adsorption kinetics and adsorption efficiencies of synthesized microcarriers because its alkaline isoelectric point is close to IGF-1. The pDA-coated microcarriers were interacted with aqueous lysozyme solutions by means of rotator. Briefly, 50 mg of the microcarriers were incubated with 10 mL of lysozyme solution ($2 \text{ mg} \cdot \text{mL}^{-1}$) under stirring at 150 rpm for 1 h. The pH of the medium adjusted by using acetate and phosphate buffer systems in own buffering ranges was varied in the range of 5.0–9.0. Effects of interaction time from 5 to 60 min on the adsorption capacity were then evaluated. The adsorbed lysozyme concentration was determined through the decrease of the concentration of lysozyme within the samples using BCA kit.

2.6. Cell Culture

ADSCs were isolated from adipose tissues obtained from BALB/c mouse (SCXX (JING) 2009-0015) using an established protocol.^[31] The animals were provided by Jilin University, Changchun, China and treated according to the NIH Guide for the Care and Use of Laboratory Animals.

Briefly, the tissues were extracted and washed with phosphate buffer saline (PBS) on a separating sieve, then treated with 0.075% collagenase type I (Gibco) for 1 h at 37°C under shaking. Cells were collected by centrifugation at 1 200 rpm, 4°C for 10 min and plated in tissue culture flasks along with Dulbecco's modified Eagle medium (DMEM, Gibco) supplemented with 10% fetal bovine serum (Gibco), $100 \text{ U} \cdot \text{mL}^{-1}$ penicillin and $100 \text{ U} \cdot \text{mL}^{-1}$ streptomycin (Sigma). After the cells were attached, the medium was removed, washed with PBS, and replaced with fresh medium. The cells were cultured to 80% confluency and then passaged for cell expansion. ADSCs of passages 2 or 3 were used for the experiments in this study.

2.6.1. Cell Proliferation

The microcarriers (pure, pDA-coated, and IGF-1-immobilized) were sterilized by immersing in 70% alcohol for 30 min. After being washed by PBS for three times and immersed in cell culture medium overnight, they were placed into 24-well plate ($20 \text{ mg} \cdot \text{well}^{-1}$) to cover the bottom of wells. 1 mL ADSCs suspension ($3 \times 10^4 \text{ mL}^{-1}$) was then seeded into each well. The plates were incubated at 37°C in a humidified 5% CO_2 atmosphere and the culture medium was replaced every 2 d. After 4 and 7 d culture, the medium was replaced by Cell Counting Kit-8 (CCK-8, Dojindo, Japan). After 2 h of incubation, the absorbance values at 450 and 600 nm were measured on a multifunctional microplate scanner (Tecan Infinite M200).

2.6.2. Confocal Laser Scanning Microscope (CLSM)

Cell morphology and colonization/proliferation were investigated by CLSM analysis. The cell/microcarriers samples were removed from the wells, rinsed twice with PBS solution, and fixed with 4% paraformaldehyde for 10 min at room temperature. After washing three times with PBS solution, the samples were incubated for 5 min with Triton X-100 (0.25% v/v) in PBS solution. Actin microfilaments were then stained with phalloidin tetramethylrhodamine B isothiocyanate (Invitrogen) diluted in BSA/PBS (1% w/v) by incubating the cell/microcarriers constructs for 30 min at room temperature. Nucleus detection was performed by using 4, 6-diamidino-2-phenylindole (DAPI, Invitrogen). DAPI stock solution was diluted in BSA/PBS, and the microcarriers/cells samples were incubated for 2 min at room temperature. The microcarriers/cells samples were then washed three times with PBS solution and observed by means of CLSM (Zeiss LSM 780).

2.6.3. Alkaline Phosphate Activity Assay

ALP activities of ADSCs incubated for 4 and 7 d were evaluated by measuring the amount of p-nitrophenol produced using p-nitrophenol phosphate substrate (pNPP) solution (Sigma). Briefly, the medium of each well was carefully removed at the end of the

incubation. Then ADSCs were washed three times with PBS and lysed in RIPA buffer before freezing at -80°C for 30 min and thawing at 37°C . 50 μL of pNPP solution for each well was added in the dark and incubated at 37°C for 30 min. The absorbance at 405 nm was read by multifunction microplate scanner. The average OD values were used to reflect the level of ALP activities correspondingly.

2.6.4. Quantitative Real-Time Polymerase Chain Reaction

ADSCs cultured on various microcarriers were incubated at 7 d and the mRNA expression of osteogenesis-related genes was quantitatively assessed using qRT-PCR technique. The total RNA was extracted using TRIzol Reagent (Invitrogen) according to the manufacturer's protocol. The concentration and purity of RNA were estimated using Nanodrop Plates (Tecan Infinite M200) and reverse transcribed using PrimeScript RT Reagent Kit with gDNA Eraser (Perfect Real Time, TaKaRa). The expression of osteogenic markers was quantified by qPCR SYBR Green Mix Kit (TaKaRa). Gene-specific primers including glyceraldehyde-3-phosphate dehydrogenase (GAPDH), anti-runt-related transcription factor 2 (RUNX2), and osteopontin (OPN) were designed using the primer design software of beacon 5.0 (Table 1). qRT-PCR was conducted by StepOnePlus Real-Time PCR System (Applied Biosystems, CA) and expression levels were obtained using threshold cycles (Ct) that were determined by the iCycler iQ Detection System software. Relative transcript quantities were calculated using the $\Delta\Delta\text{Ct}$ method. The gene GAPDH was used as a reference gene and was amplified along with the target genes from the same cDNA samples. The difference in Ct of the sample mRNA relative to GAPDH mRNA was defined as the ΔCt . The difference between the ΔCt of the control cells and the ΔCt of the cells grown on microcarriers was defined as the $\Delta\Delta\text{Ct}$. The fold change in mRNA expression was expressed as $2^{-\Delta\Delta\text{Ct}}$.

3. Results and Discussion

3.1. Characterization of Microcarriers

In this study, we mainly focused on preparing a novel functionalized PLGA/HA microcarriers by pDA coating for the affinity adsorption of IGF-1. The pDA coating on the microcarriers was achieved by oxidative polymerization of DA molecules in alkaline medium.^[32] After treatment, the surface coating can be easily distinguished by color change of the microcarriers (Figure 1a-3-d-3). Figure 1 shows the SEM images of these microcarriers. It was clear that pure PLGA microcarriers were almost spherical and had a smooth

surface. Their average diameters were also calculated to be $223.71 \pm 53.39 \mu\text{m}$. The surface roughness were found on PLGA/HA microcarriers because of the incorporation of HA crystals. After pDA coating, the surface roughness of both PLGA and PLGA/HA microcarriers increased while spherical form of the microcarriers was retained. However, PLGA/HA microcarriers exhibited more surface roughness compared to PLGA microcarriers.

The microcarriers were also analyzed with EDX. It was found that the major elements in the pure PLGA microcarriers were carbon (C) and oxygen (O). Phosphorus (P) and calcium (Ca) were only found in the EDX spectra of PLGA/HA microcarriers, which demonstrated that there were the HA crystals exposed on the microcarrier surface. After pDA coating, nitrogen (N) was found in the EDX spectra of both PLGA and PLGA/HA microcarriers, whereas N was not found in the EDX spectra of the two microcarriers without pDA coating. The EDX spectra suggested that pDA accumulation was succeeded onto the microcarriers.

The FT-IR spectra of the microcarriers were also performed to determine the pDA coating. Figure 2 shows the broad absorption band at $3000\text{--}3600 \text{ cm}^{-1}$, which represented the different types of strong hydrogen bonding interactions, including intramolecular and intermolecular --O/H--N , --O/H--O or --N/H--N . And another broad absorption band at $1500\text{--}1660 \text{ cm}^{-1}$ represented C=O stretching of amide (I), N--H bending of amide (II), stretching vibration of the quinoid (N=Q=N), and benzenoid (N--B--N) units of pDA assigned to 1646, 1566, 1603, and 1508 cm^{-1} , respectively. The spectra of PLGA/HA microcarriers showed similar changes after pDA coating. All of the variations of the FT-IR spectra further conformed that pDA was successfully fixed on the surfaces of both the PLGA and PLGA/HA microcarriers.

3.2. Protein Adsorption Studies

3.2.1. Influence of pH on Lysozyme Adsorption

It is known that pH, which influences the interactions between biological materials and solid supports, plays an important role for possible usage in biotechnological applications. Figure 3 shows the model protein adsorption curves of pDA @ PLGA and pDA @ PLGA/HA

Table 1. Sequences of primers for the qRT-PCR.

Gene	Forward primer sequence	Reverse primer sequence
RUNX2	5-GCCCTCATCTTCACTCCAAG-3t	5-GGTCAGTCAGTGCCTTTCCTC-3t
OPN	5-TCAGGACAACAACGGAAAGGG-3t	5-GGAACTTGCTTGACTATCGATCAC-3
GAPDH	5-CAACCTGGTCCTCAGTGAGC-3C	5-CGTGCCCGCTGGAGAAACCTGCC-33

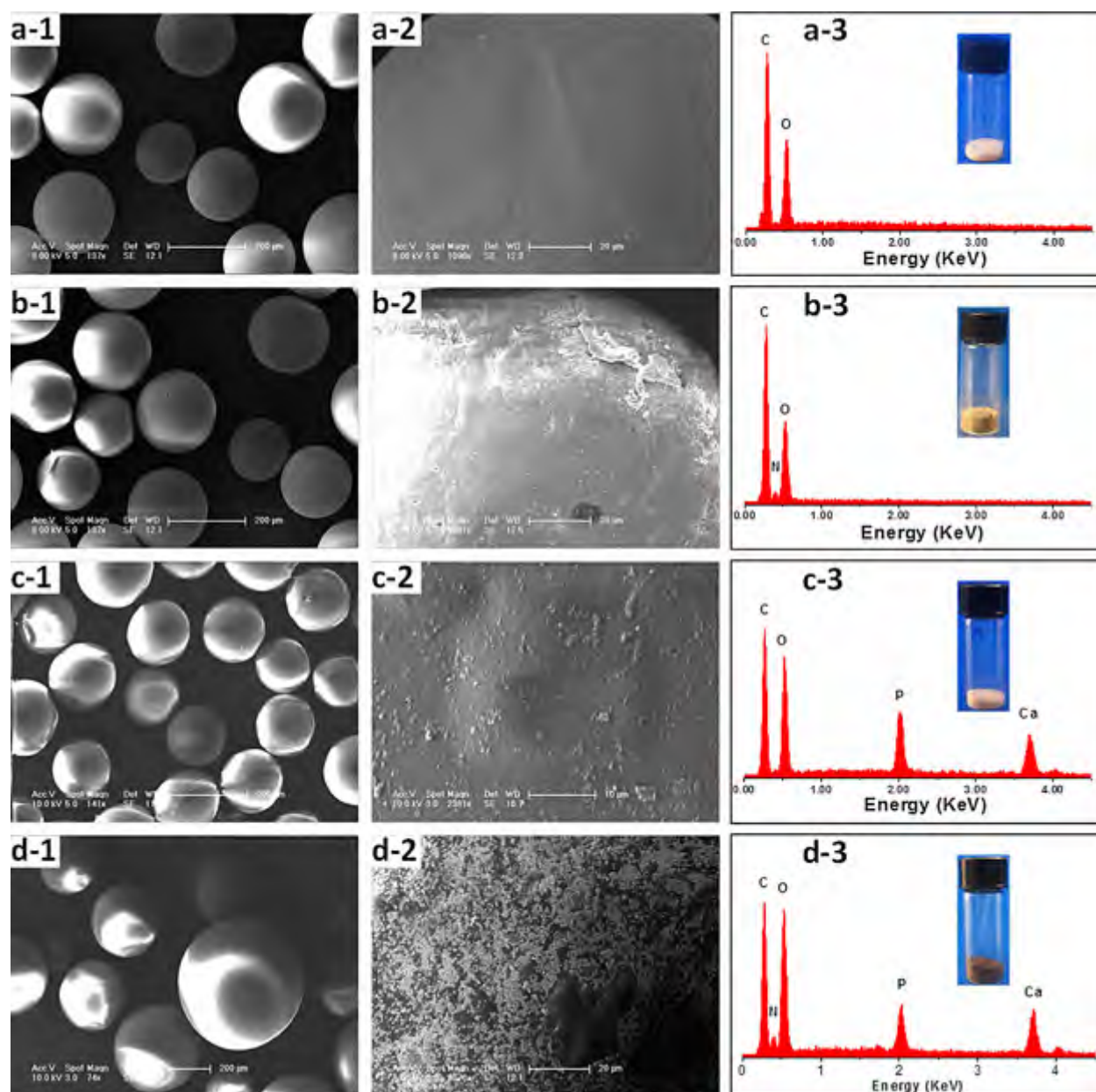


Figure 1. SEM images (1–2) and EDX (3) of PLGA (a), pDA @ PLGA (b), PLGA/HA (c), and pDA @ PLGA/HA (d) microcarriers. Bar lengths are 200 μm (a-1, b-1, c-1, and d-1), 20 μm (a-2, b-2, and d-2) and 10 μm (c-2).

microcarriers in the solutions of different pH. The lysozyme adsorption capacities were obviously increased when the pH values of solution increased from 5 to 8. The loading kinetics of lysozyme reached up to the highest when the pH value was 8.0. It was speculated that the lysozyme molecule carried a positive charge when pH below its isoelectric point (10.5). Meanwhile, oxidation and rearrangement of DA made cyclization of amino group ($-\text{NH}_2$) take place and hydroxyl ($-\text{OH}$) group remain for the polymer. Then, the hydroxyl group could

release hydrogen cations and create negative charges on the surface in neutral and basic environments. More negative charges were created after DA polymerization promoted by pH, thence more lysozymes were adsorbed on the surfaces of pDA-coating microcarriers through interactions depending on opposite charges. It is reported that the promotion of DA polymerization by pH was not obvious when pH was up to 9.0.^[26] Our research also observed that lysozyme adsorption did not increase when the pH value was up to 9.0.

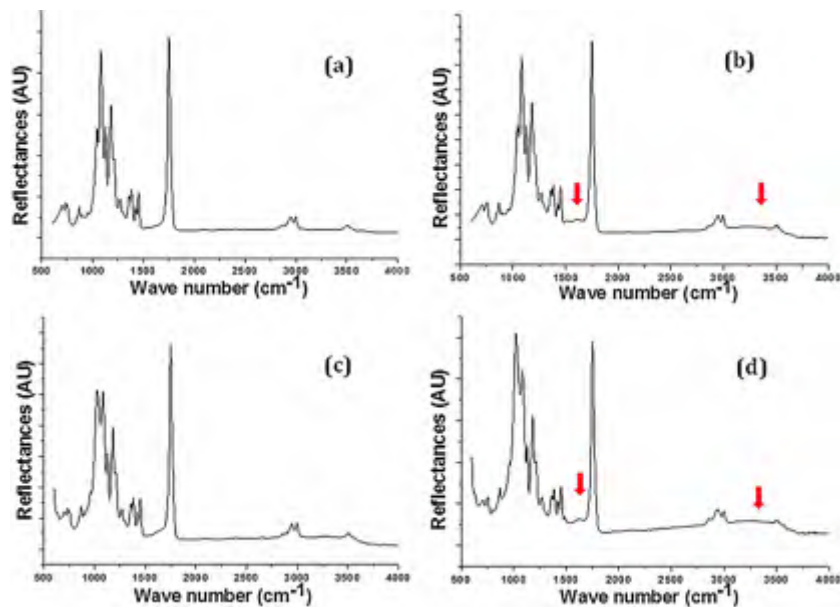


Figure 2. FT-IR spectra of PLGA (a), pDA @ PLGA (b), PLGA/HA (c), and pDA @ PLGA/HA (d) microcarriers.

3.2.2. Adsorption Rate of Lysozyme

Equilibrium adsorption time curves of lysozyme as model protein are shown in Figure 4. It is apparent that the lysozyme adsorption rates of unmodified PLGA and PLGA/HA microcarriers were obviously lower than those of pDA modified ones due to the fact that the latter ones contained functional groups of catechol. Conversely, pDA @ PLGA and pDA @ PLGA/HA microcarriers have exhibited higher lysozyme adsorption capacities, nearly 4.5 and 3.5 times of adsorption rates than those of PLGA and PLGA/HA microcarriers, respectively. It is deduced that the former is of

physical adsorption for its weak interactions between lysozyme molecules and the microcarriers, but the latter was mainly through specific interaction between catechol groups and protein moieties of lysozyme molecules. Moreover, there were relatively faster adsorption rates observed at the beginning (5 min) for pDA-coating microcarriers, and then the rates for saturation was observed in about 20 min. It may be due to a high driving force, which is the concentration difference between the liquid (i.e., the aqueous solution) and the solid (i.e., the microcarriers) phases, in the case of high lysozyme concentration.^[33] Meanwhile, the lysozyme adsorption capacities of PLGA/HA microcarriers were obviously higher than those of PLGA microcarriers and the similar trends were observed for modified microcarriers after pDA coating. It is deduced that the higher protein adsorption

capacities of nanocomposite microcarriers (PLGA/HA and pDA @ PLGA/HA) might be result from their improved surface properties and larger specific surface areas after the incorporation of HA crystals.

In Table 2, it shows that almost 2.20 mg proteins could be effectively immobilized on the surface of 50 mg pDA @ PLGA microcarriers and more proteins on the pDA @ PLGA/HA microcarriers (Figure 4). As the highest concentration of IGF-1 for surface modification was $100 \text{ ng} \cdot \text{mL}^{-1}$ in this study and the total amount of IGF-1 was 1 mg, it is speculated that the IGF-1 was nearly all fixed on the surface of the microcarriers by pDA coating.

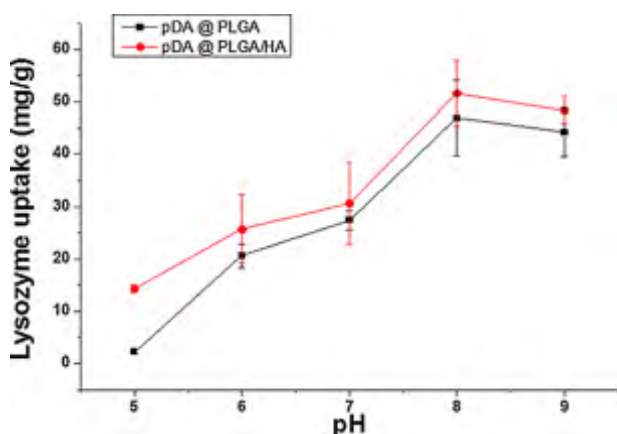


Figure 3. Effects of pH on lysozyme adsorption rates of pDA-coating microcarriers. Error bars represent standard deviation for $n = 3$.

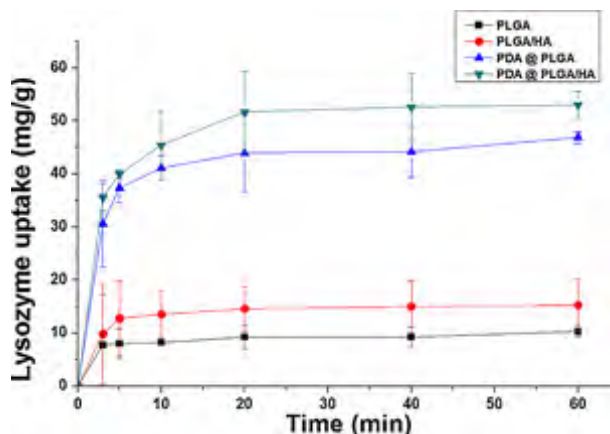


Figure 4. Lysozyme adsorption rates of microcarriers. Lysozyme concentration: $2 \text{ mg} \cdot \text{mL}^{-1}$; pH: 8; temperature: 25°C . Error bars represent standard deviation for $n = 3$.

Table 2. Protein immobilized on pDA @ PLGA microcarriers.

Peptide concentration	Solution volume [mL]	Total peptide amount [mg]	pDA @ PLGA microcarriers [mg]	Total immobilized peptide amount [mg]
2 mg · mL ⁻¹ lysozyme	10	20	50	2.20
1 ng · mL ⁻¹ IGF-1	10	0.001	50	–
10 ng · mL ⁻¹ IGF-1	10	0.1	50	–
100 ng · mL ⁻¹ IGF-1	10	1	50	–

3.3. Cell Culture

3.3.1. Cell Viability

The total population of ADSCs growing on the surface of different microcarriers at 4 and 7 d was investigated using CCK-8 assay and shown in Figure 5. As a vehicle for cell proliferation, the surface properties of microcarriers play a key role for promotion of cell adhesion and cell growth. It was clear that the OD values of cell viability showed the lowest level on the untreated PLGA microcarriers at 4 and 7 d. Compared to PLGA microcarriers, the cell proliferation on the PLGA/HA microcarriers was promoted by the incorporation of HA. Our previous study demonstrated that 10% HA could promote the adhesion on the PLGA films, due to its rough surface after HA doping.^[10] Chien et al.'s work demonstrated that cell adhesion was enhanced by pDA coating ascribed to surface immobilized serum adhesive proteins.^[22] Similar results were also found in

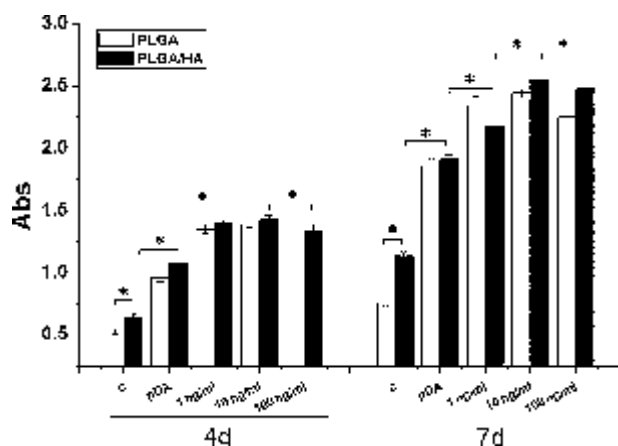


Figure 5. ADSCs proliferation on different microcarriers for 4 and 7 d. c indicated the pure microcarriers as the control, and pDA indicated the microcarriers with pDA coating. 1, 10, and 100 ng · mL⁻¹ were IGF-immobilized microcarriers treated with different concentrations of IGF-1 solution. $p < 0.05$, $n = 4$.

this study that the obvious improvements in cell proliferation at 4 and 7 d were observed on both PLGA and PLGA/HA microcarriers after pDA coating. Furthermore, the viability of cells co-cultured with IGF-1-functionalized microcarriers displayed greatly statistical differences to the pristine PLGA and PLGA/HA groups at 4 and 7 d, indicating that the peptide decorated microcarriers could promote the cell proliferation greatly. Among the groups of IGF-1-functionalized microcarriers, there were no differences in cell proliferation for PLGA or PLGA/HA treated with different density of IGF-1 solution at 4 d.

In addition, the surface immobilization of IGF-1, as low as 1 ng · mL⁻¹, markedly increased the bioactivity of the microcarriers. 10 ng · mL⁻¹ IGF-1 was most effective in the enhancement of cell proliferation among the three concentrations used in this study. However, the promotion of cell proliferation seemed to be decreased when the density of IGF-1 solution was 100 ng · mL⁻¹. IGF-1 has gained interest as a therapeutic factor either alone or in combination with other active ingredients. In vitro, IGF-1 was shown to enhance proliferation of human bone marrow stromal cells (hMSCs).^[13] In this study, IGF-1 was effectively immobilized onto the pDA-coated PLGA/HA microcarriers, and ADSCs proliferation was greatly promoted by small dose of IGF-1 immobilized onto the microcarriers. The concentration of 10 ng · mL⁻¹ was applied in the subsequent experiments.

3.3.2. Cellular Morphology and Cytoskeletal Observation

As shown in Figure 6, the morphology of the ADSCs grown on microcarriers at 4 d was further observed using CLSM by actin microfilaments (red) and nuclei (blue) staining. The nuclei staining reflected the number of cells on the surfaces of microcarriers, and actin staining reflected the structure and function of cytoskeleton of cells. The results indicated that there were more cell quantities and positive cellular interaction with the supporting structure for IGF-1-immobilized microcarriers of PLGA and PLGA/HA

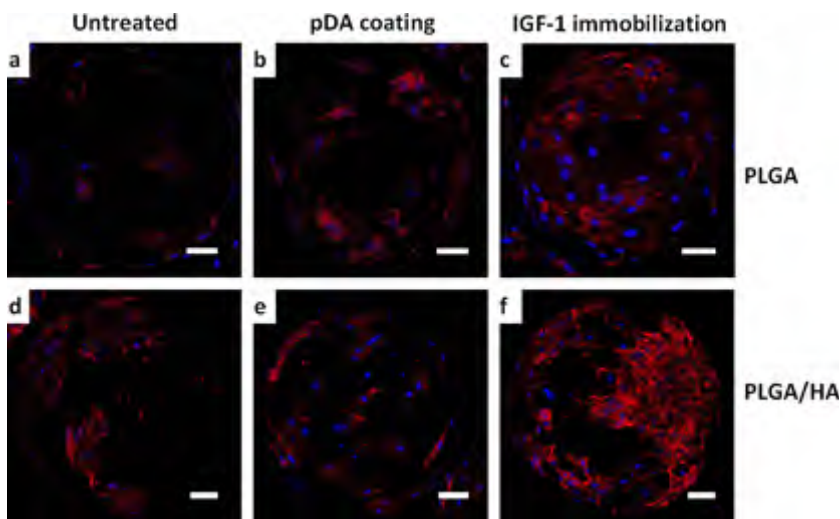


Figure 6. CLSM micrographs of PLGA (a), pDA @ PLGA (b), pDA @ PLGA/IGF-1 (c), PLGA/HA (d), pDA @ PLGA/HA (e) and pDA @ PLGA/HA/IGF-1 (f). ADSCs have been cultured on microcarriers for 4 d with actin microfilaments (phalloidin tetramethylrhodamine B isothiocyanate, red) and nucleus (DAPI, blue) staining. All scale bar lengths are 20 μm .

(Figure 6c and f). Among them, IGF-1-immobilized PLGA/HA microcarriers exhibited better cytoskeleton, indicating that both IGF-1 and HA particles are beneficial for cell growth and cell-cell communication. Compared to the untreated groups (Figure 6a and d), more adhered ADSCs were observed on pDA-coated microcarriers (Figure 6b and e). It was interesting that the gap between PLGA and PLGA/HA microcarriers was decreased after pDA coating, and it is deduced that pDA coating improved hydrophilicity significantly (Figure 6b and e). The morphological results of CLSM observation were corresponding to the CCK-8 analysis. It further supported the role of IGF-1 in promoting the attachment and proliferation of ADSCs.

3.3.3. Alkaline Phosphatase Activity

ALP activity, which peaked during the pre-osteoblast stage of differentiation,^[34] was chosen to explore the osteoinductive activity of the functionalized microcarriers. Figure 7 shows the ALP activity of ADSCs on the surfaces of the microcarriers. A great increase in ALP activity of ADSCs was found on the IGF-1-modified microcarriers, higher than those of cells on the untreated and the pDA-modified microcarriers, indicating that the cell differentiation toward osteogenesis was better on the IGF-1 modified microcarriers than other microcarriers. It was reported that IGF-1 could significantly increase ALP expression of hMSCs.^[13] Furthermore, together with some growth factors, IGF-1 showed additive effects on osteogenesis.^[16,35]

And as the primary mineral component in mature bone, 10% HA was demonstrated and that it could

increase the ALP activity of human hMSCs and induce the cells toward osteogenic differentiation.^[36] In present study, there was higher activity of ALP on the PLGA/HA microcarriers than that of the pure PLGA microcarriers at both 4 and 7 d. It indicated that the HA could also induce the ADSCs differentiating toward osteogenesis. Furthermore, there was significant difference between PLGA/HA and pDA @ PLGA/HA/IGF-1 microcarriers. The value of ALP activity on the pDA @ PLGA/HA/IGF-1 microcarriers were about 1.4 and 1.5 times as that on the PLGA/HA microcarriers at 4 and 7 d, respectively. It is deduced that the combination of IGF-1 and HA could efficiently induce the ADSCs toward osteoblasts. However, no significant difference of ALP activity of ADSCs was found on either pure microcarriers or those modified with

pDA, suggesting that pDA coating played little role on the ADSCs differentiation.

3.3.4. Quantitative Real-Time Polymerase Chain Reaction

The expression of osteogenic markers (RUNX2 and OPN) of ADSCs after 7 d of culture on these microcarriers was quantitatively analyzed using qRT-PCR and shown in Figure 8. The results demonstrated that the osteogenic gene expressions of both RUNX2 and OPN of ADSCs increased significantly when the cells were cultured on the three groups of PLGA/HA microcarriers. Among them, pDA @ PLGA/HA/IGF-1 showed the highest expression levels of RUNX2 and OPN, nearly 1.3-fold for RUNX2 and 2.9-fold for OPN higher than those of pure PLGA microcarriers. It is indicated that the HA alone or combined with IGF-1 could enhanced the osteogenic differentiation of ADSCs. It is reported that HA could promote hBMSCs osteogenic differentiation by increasing RUNX2, secreted phosphoprotein 1(SPP1), and COL-1 expression.^[36] Moreover, IGF-1, as an anabolic growth factor, could stimulate stem cells migration, survival, development, maturation, and matrix synthesis.^[14]

Although the literature suggested that pDA coating alone may promote commitment of human ADSCs to osteogenic lineage,^[29] only the expression of RUNX2 in present study was increased significantly for pDA coating alone on PLGA microcarriers without peptide immobilization. Meanwhile, compared to pure ones, there were no significant increase alone in RUNX2 expression and slight increase in OPN expression on IGF-1 immobilized alone microcarriers. Doorn et al. demonstrated that IGF-1 could increase RUNX2

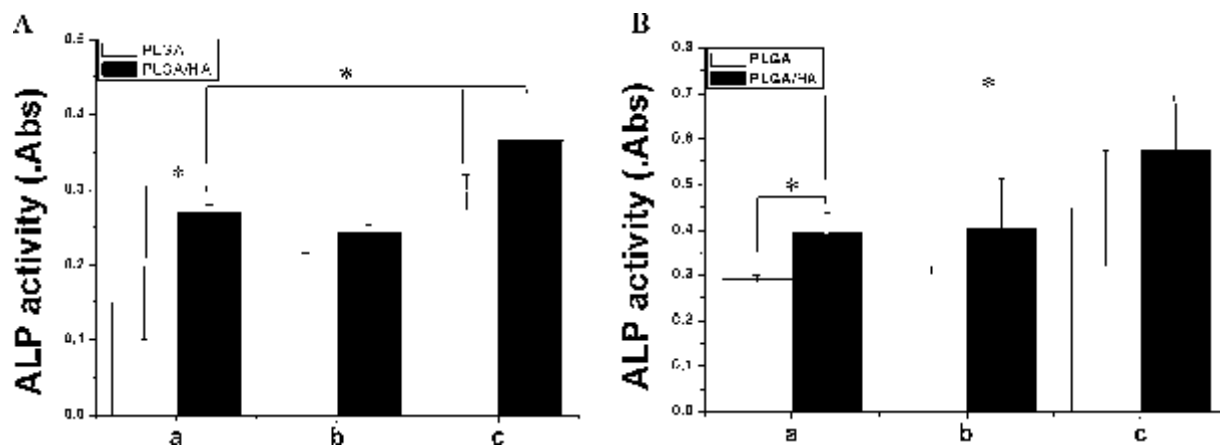


Figure 7. ALP activities of ADSCs on different microcarriers for 4 d (A) and 7 d (B) analyzed with pNPP kit (a: the pure microcarriers; b: pDA-coated microcarriers; c: IGF-immobilized microcarriers). $p < 0.05$, $n = 4$.

and OPN expression of hMSCs in vitro.^[13] While Kim et al. found that IGF-1 alone did not significantly affect the early osteoblast-associated genes of the W-20-17 cells.^[35] In this study, it was speculated that IGF-1 could, but slightly, promote the osteogenic differentiation of ADSCs. But when combined with HA, IGF-1 showed additive effects on osteogenesis.

One of the major problems in tissue engineering or cell therapy is lack of a sufficient number of cells with the appropriate phenotype for delivery to damaged or degenerated site.^[37] The microcarrier bioreactor culture system offers an attractive approach for cell amplification and enhancement of specific phenotype expression. But before construction or transplantation, the cells usually have to be harvest by enzyme digesting and their activity will be decreased. An important advantage of the biodegradable microcarriers in present study is that the cell-seeded microcarriers can be delivered directly to the sites, thus

eliminating the traditional needs for digesting and re-seeding the retrieved cells into a scaffold delivery system. The superior biodegradability of PLGA and HA nanocomposite in the forms of scaffolds has been reported in our previous studies.^[11,38] It is believed that the microcarriers of PLGA or PLGA/HA have the similar in vivo biodegradability.

On the other hand, the introduction of HA nanoparticles is important for the biodegradable PLGA microcarriers when they were designed and fabricated specifically for bone tissue engineering. Firstly, the protein adsorption and cell proliferation were increased by incorporation of HA due to improved surface properties, such as the increase of specific surface areas and surface roughness. Secondary, the levels of ALP activity and osteogenic gene expression of ADSCs were increased obviously by incorporation of HA, and the greatest effects were reached by the further combination of HA and IGF-1. However, the use of IGF-1

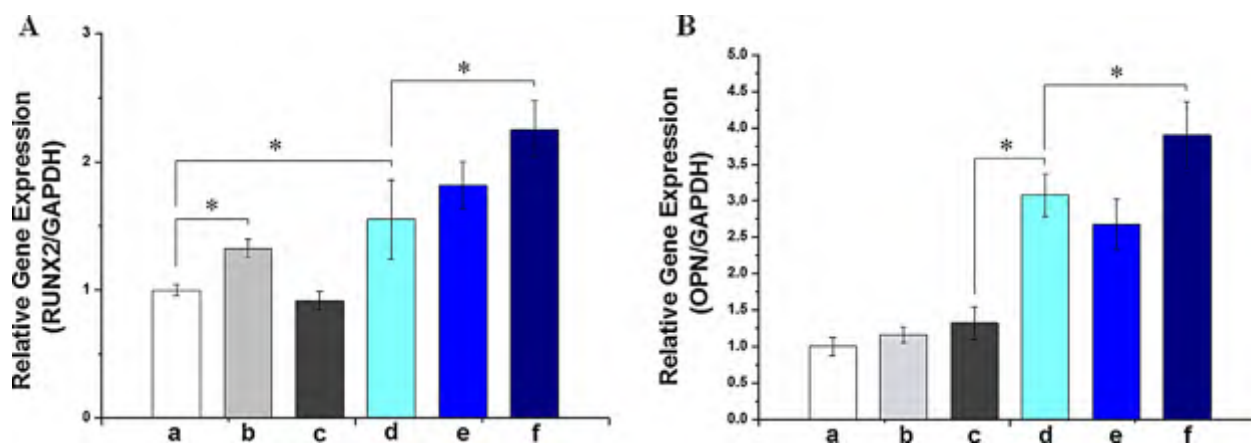


Figure 8. Quantitative real-time PCR analysis of osteogenesis-related gene expression of RUNX2 (A) and OPN (B) after ADSCs cultured for 7 d (a: PLGA, b: pDA @ PLGA, c: pDA @ PLGA/IGF-1, d: PLGA/HA, e: pDA @ PLGA/HA, f: pDA @ PLGA/HA/IGF-1). $p < 0.05$, $n = 4$.

solely can only result in the enhancement of proliferation. The results of present study indicated that the PLGA microcarriers combined with HA and IGF-1 might be an optimal way for the improvement of osteogenic differentiation of ADSCs.

Furthermore, the pDA was employed in this study for pre-modification of microcarriers, which will provide an easy approach for surface immobilization of growth factors. The advantage of pDA is that it can be easily deposited on virtually all types of inorganic and organic substrates, served as the starting points for covalent modification with desired molecules via many functional groups such as catechol, amine, and imine.^[39] DA is regarded as processing excellent biocompatibility because it is a natural molecule in the body. However, the long-term effects of stability and toxicity during the retention of pDA in the culture environment or organism should be taken into account when they were applied in tissue engineering.^[39] The clinically relevant indexes associated with pDA such as mutagenicity, teratogenicity, carcinogenicity, reproductive toxicity, and genotoxicity will be determined in our future work.

Meanwhile, the in vivo study of the cell-seeded microcarriers is necessary to verify their advantages in osteogenesis in our future work. It is expected to provide a convenient way for carrying stem cells into the site of bone defect by being injected with the assistance of hydrogels, such as collagen, alginate, or fibrinogen, or grafted to the defect combined with 3D scaffolds.

4. Conclusion

In this study, the biodegradable PLGA/HA microcarriers have been successfully fabricated by O/W emulsion with diameters of $223.71 \pm 53.39 \mu\text{m}$. And the surface roughness of microcarriers was increased because of HA incorporation. Then, the microcarriers were effectively immobilized with IGF-1 via polymerization of DA. The highly efficient protein immobilization of the microcarriers was obtained at pH 8 within 20 min. After immobilized IGF-1, the microcarriers exhibit excellent bioactivities for supporting the adhesion, proliferation, and osteogenic differentiation of ADSCs. It is expected that the novel biodegradable microcarriers would not only serve as substrates for the propagation of anchorage-dependent cells in vitro but also could be used as carriers to deliver the expanded undifferentiated or differentiated cells to the site of bone defect.

Acknowledgements: We gratefully acknowledge the financial support from the National Natural Science Foundation of China (nos. 51273195, 51203152, 51473164, and 51403197), the Joint Research Project of CAS-JSPS (no. GJHZ1519), the International

Science and Technology Cooperation Program of China (2014DFG52510), as well as the Major Project of Science and Technology of Jilin Province (20130201005GX).

Received: March 3, 2015; Revised: April 16, 2015; Published online: May 7, 2015; DOI: 10.1002/mabi.201500069

Keywords: biodegradable PLGA microcarriers; bone tissue engineering; IGF-1; nano-hydroxyapatite; polydopamine

- [1] H. H. Deboer, *Clin. Orthop. Relat. Res.* **1988**, 226, 292.
- [2] K. L. B. Brown, R. L. Cruess, *J. Bone Joint Surg. Am.* **1982**, 64, 270.
- [3] H. Shen, X. Hu, F. Yang, J. Bei, S. Wang, *Acta Biomater.* **2010**, 6, 455.
- [4] P. Zhang, H. Wu, H. Wu, Z. Lu, C. Deng, Z. Hong, X. Jing, X. Chen, *Biomacromolecules* **2011**, 12, 2667.
- [5] Z. Yang, S. Yuan, B. Liang, Y. Liu, C. Choong, S. O. Pehkonen, *Macromol. Biosci.* **2014**, 14, 1299.
- [6] A. Kodali, T. C. Lim, D. T. Leong, Y. W. Tong, *Macromol. Biosci.* **2014**, 14, 1458.
- [7] X. Shi, L. Sun, J. Jiang, X. Zhang, W. Ding, Z. Gan, *Macromol. Biosci.* **2009**, 9, 1211.
- [8] X. Shi, J. Jiang, L. Sun, Z. Gan, *Colloids Surf. B, Biointerfaces* **2011**, 85, 73.
- [9] J. M. Curran, S. Fawcett, L. Hamilton, N. P. Rhodes, C. V. Rahman, M. Alexander, K. Shakesheff, J. A. Hunt, *Biomaterials* **2013**, 34, 9352.
- [10] Y. Cui, Y. Liu, Y. Cui, X. B. Jing, P. B. A. Zhang, X. S. Chen, *Acta Biomater.* **2009**, 5, 2680.
- [11] P. Zhang, Z. Hong, T. Yu, X. Chen, X. Jing, *Biomaterials* **2009**, 30, 58.
- [12] G. Chen, Y. Xia, X. Lu, X. Zhou, F. Zhang, N. Gu, *J. Biomed. Mater. Res. Part A* **2013**, 101, 44.
- [13] J. Doorn, S. J. Roberts, J. Hilderink, N. Groen, A. van Apeldoorn, C. van Blitterswijk, J. Schrooten, J. de Boer, *Tissue Eng. Part A* **2013**, 19, 1817.
- [14] C. An, Y. Cheng, Q. Yuan, J. Li, *Ann. Biomed. Eng.* **2010**, 38, 1647.
- [15] A. Bernstein, H. O. Mayr, R. Hube, *J. Biomed. Mater. Res. Part B, Appl. Biomater.* **2010**, 92, 215.
- [16] A. Jaklenec, A. Hinckfuss, B. Bilgen, D. M. Ciombor, R. Aaron, E. Mathiowitz, *Biomaterials* **2008**, 29, 1518.
- [17] W. K. Jeong, S. W. Park, G. I. Im, *J. Biomed. Mater. Res. Part A* **2008**, 86, 1137.
- [18] G. Schmidmaier, B. Wildemann, H. Bail, M. Lucke, T. Fuchs, A. Stemberger, A. Flyvbjerg, N. P. Haas, M. Raschke, *Bone* **2001**, 28, 341.
- [19] J. Liebscher, R. Mrowczynski, H. A. Scheidt, C. Filip, N. D. Hadade, R. Turcu, A. Bende, S. Beck, *Langmuir: ACS J. Surf. Colloids* **2013**, 29, 10539.
- [20] A. L. Gao, F. Liu, L. X. Xue, *J. Membrane Sci.* **2014**, 452, 390.
- [21] J. Ryu, S. H. Ku, M. Lee, C. B. Park, *Soft Matter* **2011**, 7, 7201.
- [22] C. Y. Chien, W. B. Tsai, *ACS Appl. Mater. Interfaces* **2013**, 5, 6975.
- [23] H. Shen, X. X. Hu, F. Yang, J. Z. Bei, S. G. Wang, *Biomaterials* **2009**, 30, 3150.
- [24] Y. Ito, H. Hasuda, M. Sakuragi, S. Tsuzuki, *Acta Biomater.* **2007**, 3, 1024.
- [25] C. Wang, Y. Gong, Y. Lin, J. Shen, D. A. Wang, *Acta Biomater.* **2008**, 4, 1226.

- [26] J. Jiang, J. Xie, B. Ma, D. E. Bartlett, A. Xu, C. H. Wang, *Acta Biomater.* **2014**, *10*, 1324.
- [27] H. Lee, S. M. Dellatore, W. M. Miller, P. B. Messersmith, *Science* **2007**, *318*, 426.
- [28] R. Srikar, A. L. Yarin, C. M. Megaridis, A. V. Bazilevsky, E. Kelley, *Langmuir: ACS J. Surf. Colloids* **2008**, *24*, 965.
- [29] E. Ko, K. Yang, J. Shin, S. W. Cho, *Biomacromolecules* **2013**, *14*, 3202.
- [30] N. Zhang, T. Gao, Y. Wang, Z. Wang, P. Zhang, J. Liu, *Mater. Sci. Eng. C, Mater. Biol. Appl.* **2015**, *46*, 158.
- [31] R. Yao, R. Zhang, J. Luan, F. Lin, *Biofabrication* **2012**, *4*, 025007.
- [32] Y. Sun, Y. Deng, Z. Ye, S. Liang, Z. Tang, S. Wei, *Colloids Surf. B, Biointerfaces* **2013**, *111*, 107.
- [33] F. Yilmaz, K. Kose, M. M. Sari, G. Demirel, L. Uzun, A. Denizli, *Colloids Surf. B, Biointerfaces* **2013**, *109*, 176.
- [34] H. Cui, Y. Wang, L. Cui, P. Zhang, X. Wang, Y. Wei, X. Chen, *Biomacromolecules* **2014**, *15*, 3146.
- [35] S. Kim, Y. Kang, C. A. Krueger, M. Sen, J. B. Holcomb, D. Chen, J. C. Wenke, Y. Yang, *Acta Biomater.* **2012**, *8*, 1768.
- [36] N. H. Dormer, Y. Qiu, A. M. Lydick, N. D. Allen, N. Mohan, C. J. Berkland, M. S. Detamore, *Tissue Eng. Part A* **2012**, *18*, 757.
- [37] J. Malda, C. G. Frondoza, *Trends Biotechnol.* **2006**, *24*, 299.
- [38] Y. F. Tang, J. G. Liu, Z. L. Wang, Y. Wang, L. G. Cui, P. B. Zhang, X. S. Chen, *Chin. J. Polym. Sci.* **2014**, *32*, 805.
- [39] Y. Liu, K. Ai, L. Lu, *Chem. Rev.* **2014**, *114*, 5057.